Electronic Supplementary Information (ESI)

Carbon-Incorporated Porous Honeycomb NiCoFe Phosphide Nanospheres Derived from a MOF Precursor for Overall Water Splitting

Xijun Wei,[a] Yunhuai Zhang,[*a] Huichao He, [*b] Shuangrui Yao,[a] Li Peng, [c] Shenghuan Xiao, [a] and Peng Xiao[a,c]

[a] *College of Chemistry and Chemical Engineering, Chongqing University, Chongqing 400044, China*

[b] *State Key Laboratory of Environmental Friendly Energy Materials, School of Materials Science and Engineering, Southwest University of Science and Technology, Mianyang, Sichuan, 621010, China.*

[c] *College of Physics, Chongqing University, Chongqing 400044, China*

Experimental details

Chemicals and reagents

All the chemicals and reagents used in the experiment were of analytical grade and used without further purification. The $K_3[Fe(CN)_6]$, $Ni(NO_3)_2 \cdot 6H_2O$, $Co(NO_3)_2 \cdot 6H_2O$, KOH and $Na_3C_6H_5O_7 \cdot 2H_2O$ were all obtained from ShangHai Aladdin Biological Technology Co., Ltd.(ShangHai, China).

Synthesis process

Synthesis of $Ni_xCo_{3-x}[Fe(CN)_6]_2$ precursors

1.0 g of sodium citrate, 0.045 g of nickel nitrate and 0.045 g of cobalt nitrate were dissolved in 50 mL of deionized water (DIW) to form solution A. 0.15 g of potassium ferricyanide was dissolved in 50 mL of DIW to form solution B. Then, solutions A and B were mixed under magnetic stirring for 5 min. The obtained mixed solution was then transferred to a 50 mL Teflon-lined stainless steel autoclave. The autoclave was sealed and kept at 140 °C for 6 h in an electric oven, and naturally cooled down to room temperature. Finally, the sample was collected and rinsed several times with DI water and ethyl alcohol, followed by dried in the vacuum at 60 °C overnight.

Synthesis of carbon-incorporated porous honeycomb NiCoFe phosphide nanospheres (NiCoFeP/C)

For the synthesis of carbon-incorporated porous honeycomb NiCoFe phosphide nanocubes, the as-synthesized $Ni_xCo_{3-x}[Fe(CN)_6]_2$ precursors and NaH_2PO_2 were put in two separate porcelain boats (precursors at the downstream side of the furnace) and then putted into a quartz tube. Subsequently, the tube furnace was heated to 300 ^oC for 2 hours with a temperate ramp of 5 $^oC\ min^{-1}$ under N_2 atmosphere.

Characterization

The phases and crystal structures of the materials were characterized using the powder X-ray diffraction (XRD, Bruker D8 Advance X-ray diffractometer, Co Kα radiation, λ=1.7902 Å). The morphologies of the samples were observed by field-emission scanning electron microscopy (FESEM, JSM-7800F) and transmission

electron microscopy (TEM, JEOL-2100F). Energy dispersive spectrometer (EDS) mapping was used to further analyze the elemental compositions of the samples. X-ray photoelectron spectroscopy (XPS) analyze was conducted on a VG ESCALAB MKII spectrometer using an Mg Kα X-ray source (1253.6 eV, 120 W) at a constant analyzer.

Electrochemical measurements

The relevant electrochemical measurements were performed on a CHI 660E Electrochemical Workstation (Shanghai CH660E Instruments, China). Linear sweep voltammetry (LSV) method was performed in 1.0 M KOH solution in a standard three-electrode system at a scan rate of 5 mV s^{-1} with a graphite rod and a Ag/AgCl (Sat. KCl) electrode served as the counter and reference electrodes, respectively. The working electrodes were prepared by mixing the 5 mg active material (NiCoFeP/C, Pt/C and RuO_2), 0.44 mL of ethanol, 0.5 mL of DIW and 60 μL of 0.5 wt.% Nafion solution by ultrasonication for at least 0.5 h and 0.4 μL of the slurry was coated onto the surface of a carbon fiber paper electrode and then dried at ambient temperature. The mass loading of each electrode is around 0.28 mg cm^{-2} on the carbon fiber paper. Potentials were referenced to a reversible hydrogen electrode (RHE): E(RHE) = E(Ag/AgCl) + (0.2 + 0.059 pH)V. The long-term stability tests were performed by a continuous current density of 10 mA cm^{-2} was used. The electrochemical impedance spectroscopy (EIS) was obtained on a Zahner IM6 Electrochemical Workstation. All the data presented were corrected for iR losses and carried out at ambient temperature.

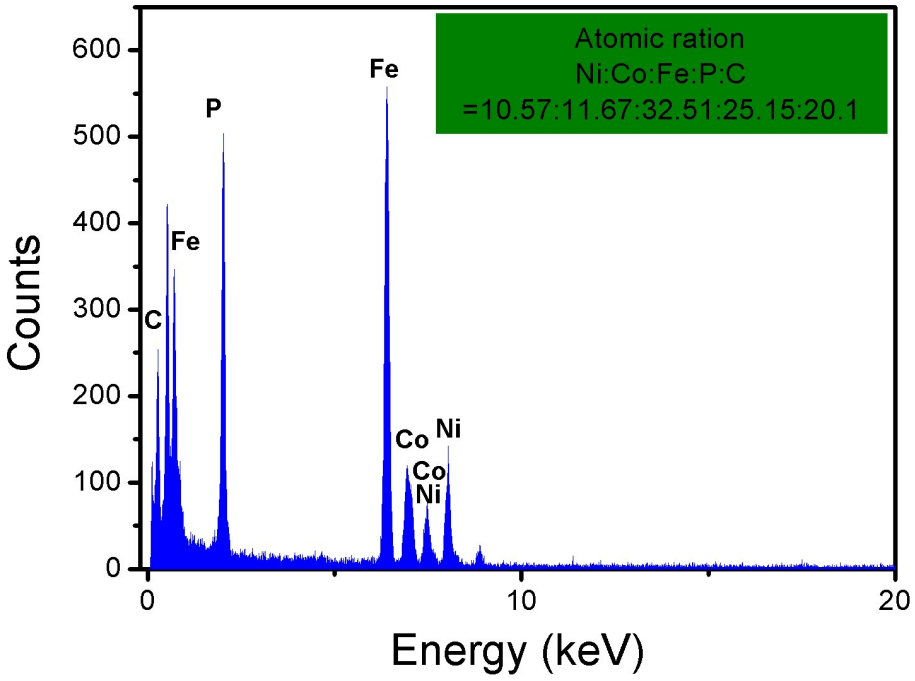

Figure S1. The EDX spectrum of NiCoFeP/C.

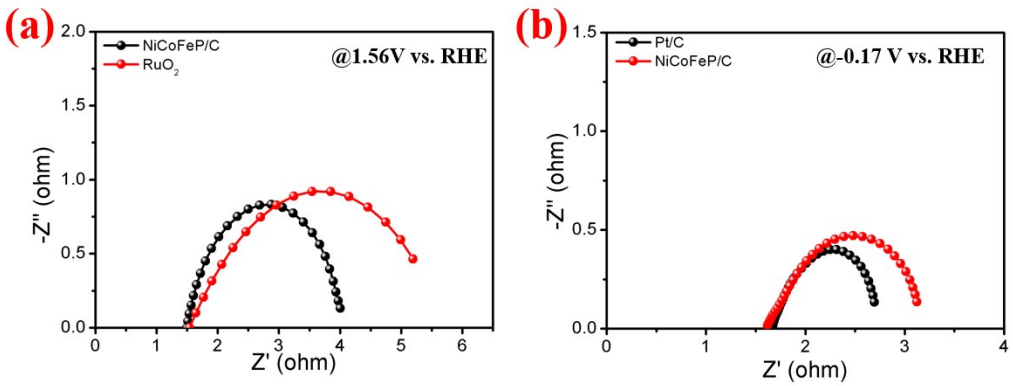

Figure S2. (a) The Nyquist plots of NiCoFeP/C and RuO_2 for OER; (b) The Nyquist plots of NiCoFeP/C and Pt/C for HER, respectively.

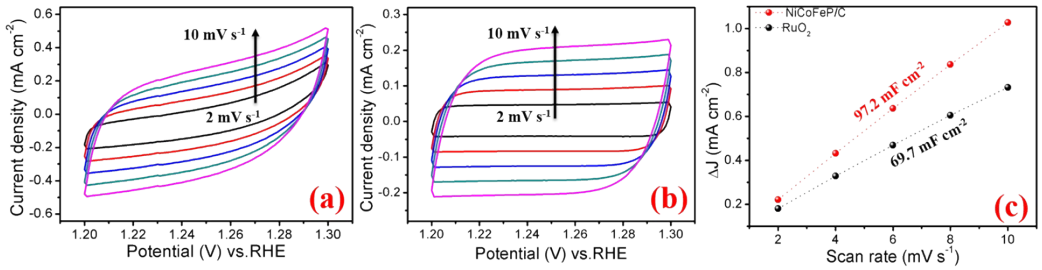

Figure S3. (a), (b) CV curves of NiCoFeP/C and RuO_2 for estimating the ECSA in OER test, respectively; (c) Corresponding capacitive currents of scan rates for NiCoFeP/C and RuO_2 in 1.0 M KOH for OER, respectively.

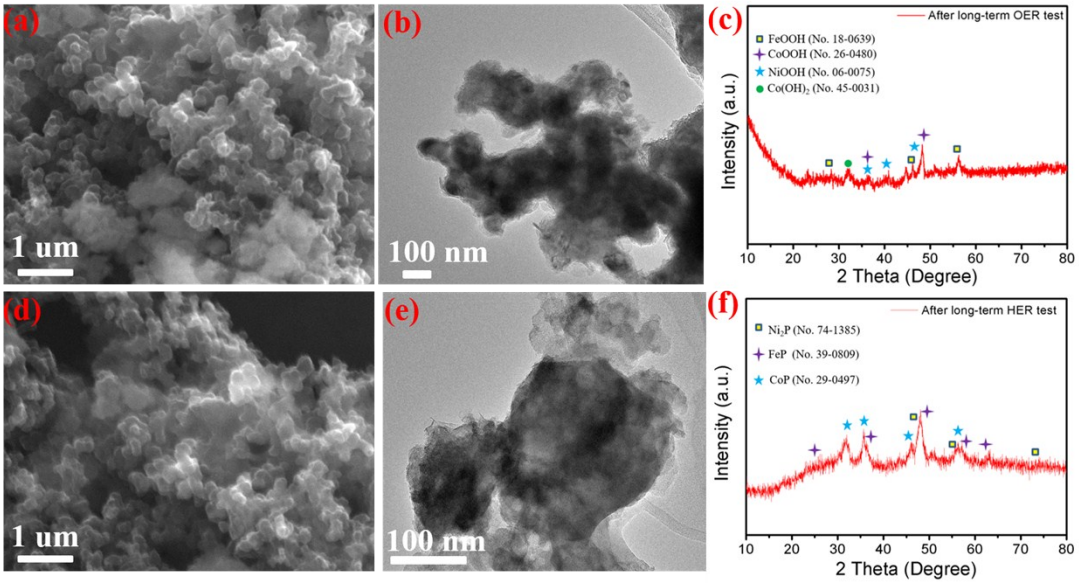

Figure S4. (a), (b), (c) The SEM, TEM images and XRD pattern of NiCoFeP/C after long-term OER test; (d), (e), (f) The SEM, TEM images and XRD pattern of NiCoFeP/C after long-term HER test , respectively.

The SEM and TEM results for NiCoFeP/C show that the morphology and structure are well retained after long-term OER and HER tests. The XRD pattern for OER exhibits that the NiCoFeP/C convert into (Ni,Co,Fe)OOH and $Co(OH)_2$.[1-4] The XRD pattern for HER shows that the phase remain unchanged.[5-9]

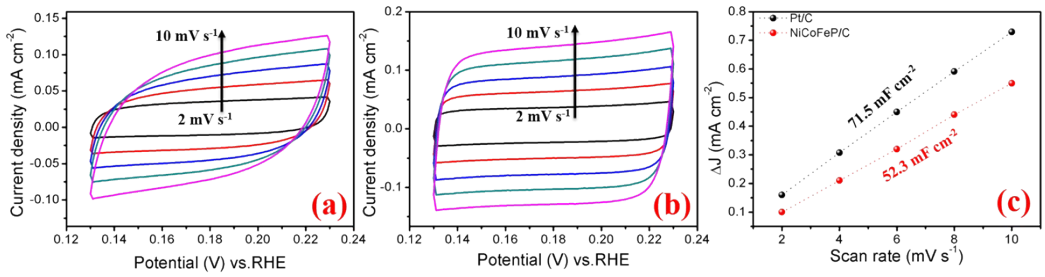

Figure S5. (a), (b) CV curves of NiCoFeP/C and Pt/C for estimating the ECSA in HER test, respectively; (c) Corresponding capacitive currents of scan rates for NiCoFeP/C and Pt/C in 1.0 M KOH for HER, respectively.

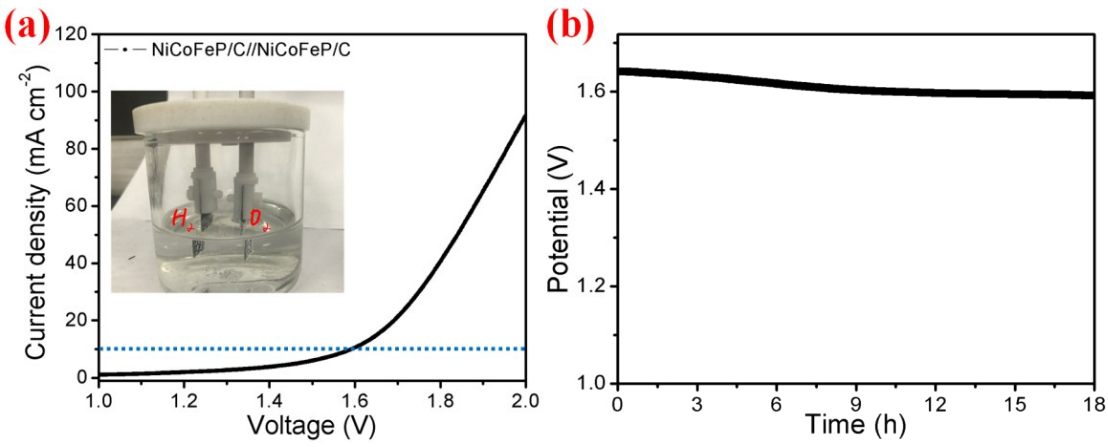

Figure S6. (a) Polarization curve of water electrolysis using NiCoFeP/C as both OER and HER electrocatalysts in a two-electrode configuration. Inset: Optical photograph showing the generation of H_2 and O_2 bubbles on the NiCoFeP/C; (b) Chronopotentiometric curve of the NiCoFeP/C for overall water splitting in a two-electrode configuration at 10 mA cm $^{-2}$ in 1 M KOH.

Table S1. Summary of various non-precious metal-based phosphides catalysts for OER.

Catalysts	**Overpotential (mV) at 10 mA cm^{-2}**	**Reference**
Ni_2P/rGO	260	J. Mater. Chem. A., **2018**, 6, 1682
FeP	288	Chem. - A Eur. J., 2015, 21, 18062– 18067
CoP/rGO	340	Chem. Sci., **2016**, 7, 1690
NiCoP/C	330	Angew. Chem. Int. Ed., **2017**, 56, 3897–3900
CoP/Co_2P	317	Nanoscale., **2018**,10, 21019-21024
CoP/PNC	300	Carbon., **2019,** 144, 464-471
$Ni_{59}Cu_{19}P_9$	318	Applied Catalysis B: Environmental., **2018**, 237, 409–415
$Ni_{0.6}Co_{1.4}P$	300	Adv. Funct. Mater., **2018**, 28,

		1706008
NiCoFeP/C	**270**	**This work**

Table S2. Summary of various non-precious metal-based phosphides catalysts for HER.

Catalysts	**Overpotential (mV) at -10 mA cm^{-2}**	**Reference**
Ni_2P/rGO	142	J. Mater. Chem. A, **2018**, 6, 1682
CoP/NC	204	Carbon., **2019**, 144, 464-471
FeP	194	Chem. Commun., **2016**, 52, 2819–2822
Ni_2P/GC	220	Energy Environ. Sci., **2015**, 8, 2347–2351
CoNiP/NF	155	Chem. Commun., **2015**, 51, 11626–11629
$Ni_{12}P_5$/NF	170	ACS Catal., **2017**, 7, 103–109
CoP/CC	209	J. Am. Chem. Soc., **2014**, 136, 7587–7590.
NiCoFeP/C	**149**	**This work**

References

1. F. Hu, S. Zhu, S. Chen, Y. Li, L. Ma et al., Adv. Mater. 2017, 29, 1606570.
2. T. Wang, G. Nam, Y. Jin, X. Wang, P. Ren et al., Adv. Mater. 2018 30, 1800757.
3. J. H Lin, Y. T. Yan, C. Li, X. Q. Si, H. H. Wang, J. L. Qi, J. Cao, Z. X. Zhong, W. D. Fei, J. C. Feng, Nano-Micro Lett., 2019, 11:55.
4. P. He, X. Y. Yu, X. W. (David) Lou, Angew. Chem. Int. Ed. 2017, 56, 3897–3900.
5. R. Zhang, J. Huang, G. L. Chen, W. Chen, C. S. Song, C. R. Li, K. Ostrikov (Ken), Applied Catalysis B: Environmental., 2019, 254, 414–423.
6. R. Boppella, J. W. Tan, W. Yang, J. Moon, Adv. Funct. Mater. 2019, 29, 1807976.
7. J. H. Chen, J, W. Liu, J. Q. Xie, H. Q. Ye, X. Z. Fu, R. Sun, C. P. Wong, Nano Energy., 2019, 56, 225–233.
8. J. G. Wang, W. Hua, M. Y. Li, H. Y. Liu, M. H. Shao, B. Q. Wei, ACS Appl. Mater. Interfaces., 2018, 10, 41237−41245.
9. C. L. Liu, G. Zhang, L.Yu, J. H. Qu, H. J. Liu, Small., 2018, 14, 1800421.